

An image encryption algorithm based on chaotic Lorenz system and novel primitive polynomial S-boxes

Temadher Alassiry Al-Maadeed¹, Iqtadar Hussain¹, Amir Anees², M. T. Mustafa¹

¹*Department of Mathematics, Statistics and Physics, Qatar University, Doha, 2713, Qatar*

²*Department of Computer Science and Information Technology, La Trobe University, Melbourne, Australia*

t.alassiry@qu.edu.qa, iqtadarqau@qu.edu.qa, a.anees@latrobe.edu.au, tahir.mustafa@qu.edu.qa

Abstract

Nowadays, the chaotic cryptosystems are gaining more attention due to their efficiency, the assurance of robustness and high sensitivity corresponding to initial conditions. In literature, on one hand there are many encryption algorithms that only guarantee security while on the other hand there are schemes based on chaotic systems that only promise the uncertainty. Due to these limitations, each of these approaches cannot adequately encounter the challenges of current scenario. Here we take a unified approach and propose an image encryption algorithm based on Lorenz chaotic system and primitive irreducible polynomial S-boxes. First, we propose 16 different S-boxes based on projective general linear group and 16 primitive irreducible polynomials of Galois field of order 256, and then utilize these S-boxes with combination of chaotic map in image encryption scheme. Three chaotic sequences can be produced by the Lorenz chaotic system corresponding to variables x , y and z . We construct a new pseudo random chaotic sequence k_i based on x , y and z . The plain image is encrypted by the use of chaotic sequence k_i and XOR operation to get a ciphered image. To demonstrate the strength of presented image encryption, some renowned analyses as well as MATLAB simulations are performed.

Keywords: Lorenz System, Chaos, Substitution box, image encryption, cryptanalysis.

1 Introduction

Last decade is considered as a remarkable era for secure communication and image processing. In wireless communication, protection of digital data like text, sound, image and video has increased importance because multimedia elements have taken hold on many important fields like electronic commerce, banking industry, law enforcement agencies requirements and personal data. The performance of old cryptosystems for image encryption is poor in encryption of bulk sized data [1, 2]. To tackle this problem, new schemes based on chaos for image encryption have been developed. In [3, 4], Amigo et. al., and Jakimoski, have shown a link between secure communication and chaos theory. They said chaotic maps could achieve some basic requirements of secure communication like randomness, robustness and sensitivity to initial conditions. In [5, 6], Ott and Alvarez have observed that values breded by chaotic maps can be regained based on initial conditions but extremely erratic, and this kind of behavior is valuable for cryptosystems. Based on these properties, some cryptographers have proposed novel cryptosystems in [7, 8]. Pseudorandom number generator based on chaotic

maps is one of the emerging field nowadays and can be utilized in different cryptosystems to get more security [9, 10].

Substitution box (S-box) is a fundamental component in symmetric key algorithms which implement substitution. Substitution boxes are building blocks of symmetric cryptosystems. The substitution tables (S-boxes) play a crucial part in the encryption algorithms in order to meet the definition of a perfect security. Sometime big structures like S-box slowdown the processing of the encryption in a scenario where big data processing is required, the main reason is the complexity of that system and this kind of negative effect reduce the utility of that encryption algorithm in practical communication. In literature, there are many chaotic schemes that are using one or multiple (S-boxes) to get more security. There is no doubt that when one will use S-box, the confusion creating ability of that algorithm between ciphertext and secret key will improve but it will definitely reduce the encryption speed [11–29]. Here, we propose an image encryption algorithm that builds on chaotic maps and S-boxes. First, we propose novel 16 different S-boxes based on 16 different primitive irreducible polynomials of Galois field of order 256 and projective general linear group, then the proposed S-boxes are utilized in image encryption. The focus is to construct an efficient and secure image encryption scheme building on straightforward and less complex steps, employing chaotic Lorenz system.

Some basic definitions of mathematical background for cryptography and details of chaotic map are given in Section 2. The detailed description of image encryption algorithm proposed in this work is given in Section 3. Section 4 depicts the outcomes of simulation and different analyses. The conclusion of whole scheme is given in Section 5.

2 Basic Definitions

The structural units of designed image encryption technique are briefly discussed in this section. First, an introduction to the Galois field and its primitive irreducible polynomials is presented which is followed by the basics of Projective General Linear Group. Next, the comprehensive description of chaotic Lorenz map is given.

2.1 Galois field and its primitive irreducible polynomials

It is known from the theory of Galois field that if p is a non-zero element of a Principle Ideal Domain (PID) \mathbf{R} , then $\frac{\mathbf{R}}{p}$ will be a field if p is irreducible. Therefore, for a prime p and $q = p^n$, the finite field of order q can be given as $\mathbf{GF}(q) = \mathbf{GF}(p^n)$. The polynomial extension $\mathbf{R}[x]$ of intergral domain \mathbf{R} is also intergral domain, therefore, in case of polynomial extension $\mathbf{R}[x]/\langle p(x) \rangle$ will be a field structure when $p(x)$ is primitive irreducible polynomial, where $\langle p(x) \rangle$ is a maximal ideal.

$$(2.1) \quad \mathbf{GF}(q) = \frac{\mathbf{GF}(p)[x]}{\langle m(x) \rangle}$$

with $m(x)$ denoting a monic primitive irreducible polynomial of degree n in Galois field $\mathbf{GF}(p^n)$. An example of above formula is as follows:

$$(2.2) \quad \mathbf{GF}(2^8) = \frac{\mathbf{GF}(2)[x]}{\langle x^8 + x^7 + x^6 + x^5 + x^4 + x^2 + 1 \rangle}$$

$$\mathbf{GF}(2^8) = \left\{ a_1 + a_2x + a_3x^2 + a_4x^3 + a_5x^4 + a_6x^5 + a_7x^6 + a_8x^7 + \langle m(x) \rangle \mid a_i \in \mathbf{GF}(2) \right\}$$

The elements of $\mathbf{GF}(2^8)$ can be represented by a polynomial of degree 8 and $\langle m(x) \rangle$ is the maximal ideal generated by monic irreducible polynomial, when the degree of polynomial will exceed from 7 this maximal ideal will absorb it. Now, the question is how many different irreducible polynomials are there corresponding to any Galosi field $\mathbf{GF}(p^n)$. The formula to find all irreducible polynomials is as follows:

$$(2.3) \quad \frac{1}{n} \sum_{d|n} \mu(d) P^{n/d}$$

By using above formula, it can be seen in Table 1, that there are 30 irreducible polynomials for $\mathbf{GF}(2^8)$. But for the construction of Galosi field which can generate its non-zero elements we need primitive irreducible polynomials. In Table 1, we have shown that out of 30 irreducible polynomials 16 are primitive irreducible. We have used Rabin's test to find 30 irreducible polynomials, Rabin's test is as follows:

Theorem 2.1. *Let p_1, p_2, \dots, p_k be all the prime divisors of n , and denoted $n_i = n/p_i$, for $1 \leq i \leq k$. A polynomial $f \in \mathbf{F}_q[x]$ of degree n is irreducible in $\mathbf{F}_q[x] \Leftrightarrow \gcd(f, x^{q^{n_i}} - x \text{ mod } f) = 1$ for $1 \leq i \leq k$, and f divides $x^{q^n} - x$.*

A polynomial that generates all elements of an extension field from a base field is called a primitive polynomial. It is worth noting that the primitive polynomials are irreducible polynomials as well. There exists a primitive polynomial of degree n over $\mathbf{GF}(q)$ for any prime or prime power q and any positive integer n . There are

$$(2.4) \quad a_q(n) = \frac{\phi(q^n - 1)}{n}$$

primitive polynomials over $\mathbf{GF}(q)$, where $\phi(n)$ is the totient function.

Theorem 2.2. *A polynomial of degree n over the finite field $\mathbf{GF}(2)$ is primitive if it has polynomial order $2^n - 1$.*

Theorem 2.1, yields 30 irreducible polynomial of Table 1. The next question is how to get 16 primitive irreducible polynomials from these 30 irreducible polynomials. The procedure is explained through an example of $GF(2^4)$.

$$(2.5) \quad \mathbf{GF}(2^4) = \frac{\mathbf{GF}(2)[x]}{\langle x^4 + x^3 + 1 \rangle}$$

There are two primitive irreducible polynomials for $\mathbf{GF}(2^4)$. The process to check whether an irreducible polynomial is primitive irreducible or not is shown in the example and counter example below.

Suppose $f(x) = x^4 + x^3 + 1$ is an irreducible polynomial. Let α be the root of $f(x)$. If α is the root of $f(x)$ then we have

$$(2.6) \quad f(\alpha) = \alpha^4 + \alpha^3 + 1 = 0$$

$$(2.7) \quad \alpha^4 = \alpha^3 + 1$$

8 degree polynomials of $\mathbf{GF}(2^8)$	Irreducible	Prim. irreducible
$x^8 + x^7 + x^5 + x^4 + 1$	Yes	No
$x^8 + x^4 + x^3 + x^2 + 1$	Yes	Yes
$x^8 + x^5 + x^3 + x^1 + 1$	Yes	Yes
$x^8 + x^7 + x^6 + x^4 + x^3 + x^2 + 1$	Yes	No
$x^8 + x^6 + x^5 + x^4 + x^2 + x^1 + 1$	Yes	No
$x^8 + x^7 + x^6 + x^5 + x^4 + x^3 + 1$	Yes	No
$x^8 + x^5 + x^3 + x^2 + 1$	Yes	Yes
$x^8 + x^6 + x^4 + x^3 + x^2 + x^1 + 1$	Yes	Yes
$x^8 + x^4 + x^3 + x + 1$	Yes	No
$x^8 + x^7 + x^6 + x^1 + 1$	Yes	Yes
$x^8 + x^6 + x^5 + x^2 + 1$	Yes	Yes
$x^8 + x^6 + x^5 + x^4 + x^3 + x^1 + 1$	Yes	No
$x^8 + x^7 + x^2 + x^1 + 1$	Yes	Yes
$x^8 + x^7 + x^5 + x^4 + x^3 + x^2 + 1$	Yes	No
$x^8 + x^7 + x^3 + x^2 + 1$	Yes	Yes
$x^8 + x^7 + x^6 + x^5 + x^4 + x^2 + 1$	Yes	Yes
$x^8 + x^5 + x^4 + x^3 + x^2 + x^1 + 1$	Yes	No
$x^8 + x^7 + x^6 + x^5 + x^2 + x^1 + 1$	Yes	Yes
$x^8 + x^7 + x^6 + x^4 + x^2 + x^1 + 1$	Yes	No
$x^8 + x^6 + x^3 + x^2 + 1$	Yes	Yes
$x^8 + x^7 + x^4 + x^3 + x^2 + x^1 + 1$	Yes	No
$x^8 + x^7 + x^6 + x^3 + x^2 + x^1 + 1$	Yes	Yes
$x^8 + x^7 + x^6 + x^5 + x^4 + x^1 + 1$	Yes	No
$x^8 + x^6 + x^5 + x^1 + 1$	Yes	Yes
$x^8 + x^5 + x^4 + x^3 + 1$	Yes	No
$x^8 + x^6 + x^5 + x^3 + 1$	Yes	Yes
$x^8 + x^7 + x^5 + x^1 + 1$	Yes	No
$x^8 + x^6 + x^5 + x^4 + 1$	Yes	Yes
$x^8 + x^7 + x^3 + x^1 + 1$	Yes	No
$x^8 + x^7 + x^5 + x^3 + 1$	Yes	Yes

Table 1: Irreducible and primitive irreducible polynomials corresponding to $\mathbf{GF}(2^8)$.

Because the coefficients of polynomial are in $\mathbf{GF}(2)$, that is why $-1 = +1$.

$$(2.8) \quad \alpha^5 = \alpha^4 + \alpha = \alpha^3 + 1 + \alpha = \alpha^3 + \alpha + 1$$

$$(2.9) \quad \alpha^6 = \alpha^4 + \alpha^2 + \alpha = \alpha^3 + 1 + \alpha^2 + \alpha = \alpha^3 + \alpha^2 + \alpha + 1$$

$$(2.10) \quad \alpha^7 = \alpha^4 + \alpha^3 + \alpha^2 + \alpha = \alpha^3 + 1 + \alpha^3 + \alpha^2 + \alpha = \alpha^2 + \alpha + 1$$

Where $2\alpha^3 = 0$ due to $GF(2)$.

$$(2.11) \quad \alpha^8 = \alpha^3 + \alpha^2 + \alpha$$

$$(2.12) \quad \alpha^9 = \alpha^4 + \alpha^3 + \alpha^2 = \alpha^3 + 1 + \alpha^3 + \alpha^2 = \alpha^2 + 1$$

$$(2.13) \quad \alpha^{10} = \alpha^3 + \alpha$$

$$(2.14) \quad \alpha^{11} = \alpha^4 + \alpha^2 = \alpha^3 + 1 + \alpha^2 = \alpha^3 + \alpha^2 + 1$$

$$(2.15) \quad \alpha^{12} = \alpha^4 + \alpha^3 + \alpha = \alpha^3 + 1 + \alpha^3 + \alpha = \alpha + 1$$

$$(2.16) \quad \alpha^{13} = \alpha^2 + \alpha$$

$$(2.17) \quad \alpha^{14} = \alpha^3 + \alpha^2$$

$$(2.18) \quad \alpha^{15} = \alpha^4 + \alpha^3 = \alpha^3 + 1 + \alpha^3 = 1$$

It can be seen in above example that we are getting $\alpha^{15} = 1$, and the order of $\mathbf{GF}(2^4)$ is 16. This means $f(x) = x^4 + x^3 + 1$ is a primitive polynomial because it is generating all non-zero elements of $\mathbf{GF}(2^4)$. Here α , the root of primitive polynomial, is known as primitive element. In other words, because \mathbf{GF} is also a cyclic group so α is the generator. All irreducible polynomials are not primitive, to show this fact a counter example is given below.

Suppose $f'(x) = x^4 + x^2 + 1$ is an irreducible polynomial. Let β be the root of $f(x)$. If β is the root of $f'(x)$ then we have

$$(2.19) \quad f'(\beta) = \beta^4 + \beta^2 + 1 = 0$$

$$(2.20) \quad \beta^4 = \beta^2 + 1$$

Because the coefficients of polynomial are in $\mathbf{GF}(2)$, that is why $-1 = +1$.

$$(2.21) \quad \beta^5 = \beta^3 + \beta$$

$$(2.22) \quad \beta^6 = \beta^4 + \beta^2 = \beta^2 + 1 + \beta^2 = 2\beta^2 + 1 = 1$$

It can be seen that $f'(x) = x^4 + x^2 + 1$ is irreducible but not primitive, because it is not generating all non-zero elements of $\mathbf{GF}(2^4)$. Similarly, in Table 1, we obtain all primitive irreducible polynomials from irreducible polynomials.

2.2 Projective General Linear Group (PGL)

The Projective General Linear Group (PGL) defined as the group acting on $\bar{F} = \mathbf{GF}(p^n) \cup \{\infty\}$ is the group of all transformations and is denoted by $PGL(2, \mathbf{GF}(p^n))$. With the standard understanding about ∞ , $PGL(2, \mathbf{GF}(p^n))$ is the set of all linear fractional transformations (LFT) of $\bar{F} = \mathbf{GF}(p^n) \cup \{\infty\}$,

$$(2.23) \quad PGL(2, \mathbf{GF}(p^n)) = \left\{ g : \bar{F} \rightarrow \bar{F} \mid g(z) = \frac{az+b}{cz+d}, a, b, c, d \in \mathbf{GF}(p^n), ad - bc \neq 0 \right\}$$

Linear fractional transformation $g(z)$ is shortly denoted by LFT. We study a special class of maps

$$(2.24) \quad f : PGL(2, \mathbf{GF}(2^8)) \times \mathbf{GF}(2^8) \rightarrow \mathbf{GF}(2^8)$$

A LFT of $PGL(2, \mathbf{GF}(2^8)) \times \mathbf{GF}(2^8)$ is a map of the form $g(z) = \frac{az+b}{cz+d}$, $a, b, c, d \in \mathbf{GF}(2^8)$ with $ad - bc \neq 0$

This transformation is depending on the invertible 2×2 matrix $\begin{pmatrix} a & b \\ c & d \end{pmatrix}$

2.3 Chaotic Lorenz System

The idea of defining the chaotic dynamics with the help of chaotic maps is a big breakthrough in the field of dynamical systems. The mathematical modelling related to atmospheric convection was presented by E. Lorenz [13, 14] through the system of chaotic differential equation given by

$$(2.25) \quad \frac{dx}{dt} = a(y - x)$$

$$(2.26) \quad \frac{dy}{dt} = bx - y - xz$$

$$(2.27) \quad \frac{dz}{dt} = xy - cz$$

with the variables x, y and z in the intervals $-60 \leq x \leq 60$, $-60 \leq y \leq 60$, $-60 \leq z \leq 60$. For chaotic behavior, the values for parameters a, b , and c respectively are $a = 10$, $b = 28$ and $c = 8/3$.

3 Primitive irreducible polynomial S-boxes

Now from the above linear transformation, we have;

$$f_i : PGL\left(2, GF(2^8) = \frac{GF(2)[x]}{\langle p_i(x) \rangle}\right) \times \left(GF(2^8) = \frac{GF(2)[x]}{\langle p_i(x) \rangle}\right) \rightarrow \left(GF(2^8) = \frac{GF(2)[x]}{\langle p_i(x) \rangle}\right)$$

where $p_i(x)$, $i = 1, 2, 3, \dots, 16$ are set of primitive irreducible polynomials of Table 1 for $GF(2^8)$. Therefore, we have 16 different f_i , where $i = 1, 2, 3, \dots, 16$ to construct 16 different S-boxes with fixed $a, b, c, d \in GF(2^8)$. The order of $PGL(2, GF(2^8))$ is 16776960, therefore one can construct huge number of S-boxes by changing $a, b, c, d \in GF(2^8)$. In this section, we

have given an example of creating one S-box using $a = 32, b = 22, c = 11, d = 8 \in GF(2^8)$ and $p_1(x) = x^8 + x^4 + x^3 + x^2 + 1$. In polynomial form, $a = x^5, b = x^4 + x^2 + x, c = x^3 + x + 1, d = x^3$. Here it must be noted that the sign $+$ indicates XOR operation.

$$(3.28) \quad f_1(z) = \frac{(x^5)(z) + (x^4 + x^2 + x)}{(x^3 + x + 1)(z) + (x^3)}.$$

For $z = 0$

$$f_1(0) = \frac{(x^5)(0) + (x^4 + x^2 + x)}{(x^3 + x + 1)(0) + (x^3)} = \frac{x^4 + x^2 + x}{x^3} = \frac{\mu^{239}}{\mu^3} = \mu^{239-3-1} = \mu^{237} = 237$$

where $\mu^{239} = \mu^4 + \mu^2 + \mu, \mu^3 = x^3$ based on $p_1(x) = x^8 + x^4 + x^3 + x^2 + 1$. It is to be noted that corresponding to different primitive polynomials $p_i(x)$ of $GF(2^8)$ these values of μ power will be different.

For $z = 1$

$$f_1(1) = \frac{(x^5)(1) + (x^4 + x^2 + x)}{(x^3 + x + 1)(1) + (x^3)} = \frac{x^5 + x^4 + x^2 + x}{2x^3 + x + 1} = \frac{x^5 + x^4 + x^2 + x}{x + 1} = \frac{\mu^{249}}{\mu^{25}} = \mu^{249-25-1} = \mu^{225} = 225$$

where $\mu^{249} = \mu^5 + \mu^4 + \mu^2 + \mu, \mu^{25} = \mu + 1$ based on $p_1(x) = x^8 + x^4 + x^3 + x^2 + 1$

For $z = 2$

$$(3.29) \quad f_1(2) = \frac{(x^5)(2) + (x^4 + x^2 + x)}{(x^3 + x + 1)(2) + (x^3)} = \frac{(x^5)(x) + (x^4 + x^2 + x)}{(x^3 + x + 1)(x) + (x^3)} = \frac{x^6 + x^4 + x^2 + x}{x^4 + x^3 + x^2 + x}$$

$$= \frac{x^5 + x^4 + x^2 + x}{x + 1} = \frac{\mu^{219}}{\mu^{76}} = \mu^{219-76-1} = \mu^{144} = 144$$

where $\mu^{219} = \mu^6 + \mu^4 + \mu^2 + \mu, \mu^{76} = \mu^4 + \mu^3 + \mu^2 + \mu$ based on $p_1(x) = x^8 + x^4 + x^3 + x^2 + 1$. Similarly, for $z = 3, 4, 5, \dots, 255$ all the elements can be constructed corresponding to primitive irreducible polynomial $p_1(x) = x^8 + x^4 + x^3 + x^2 + 1$. Table 2 displays all the elements of $p_1(x)$ S-box.

3.1 Analysis for assessing the S-box strength

The analysis section focuses on determining the cryptographic strength of the designed S-box through appropriate standard checks. The strength analysis of the designed S-boxes is carried out by employing the commonly used standard criteria constituting bijectivity, nonlinearity, bit independence criterion (BIC), strict avalanche criterion (SAC), differential approximation probability (DP), and linear approximation probability (LP). The reader is referred to [30] for definitions and important characteristics of these criteria. Table 3 presents the outcome of the strength analyses for our proposed S-boxes with different Primitive polynomial of $GF(2^8)$.

4 Proposed algorithm for image encryption cryptosystem

For encryption of the digital material, a pseudorandom sequence generator needs to be developed for transforming the real outputs of chaotic Lorenz system into a digital sequence.

	0	1	2	3	4	5	6	7	8	9	10	11	12	13	14	15
0	237	225	144	236	211	25	147	20	185	127	132	195	123	136	197	170
1	109	112	61	84	183	4	186	54	234	121	177	129	215	48	41	1
2	162	228	194	150	141	175	74	91	70	50	47	85	176	40	34	102
3	119	223	202	206	7	22	98	158	190	148	69	30	38	113	179	224
4	131	104	165	178	106	169	174	116	26	154	21	90	65	157	76	64
5	45	5	253	86	172	124	180	67	247	115	42	118	217	240	189	192
6	199	12	6	125	216	254	251	231	210	227	126	160	151	107	73	139
7	77	122	188	8	16	232	153	111	143	203	24	39	95	99	78	182
8	89	213	241	171	81	9	72	13	105	205	3	59	120	245	35	168
9	137	27	66	97	79	71	55	226	201	187	214	239	80	2	208	255
10	63	156	249	135	83	248	110	140	29	163	155	219	184	49	68	173
11	200	10	149	51	23	57	157	14	94	58	15	209	18	103	193	142
12	133	11	56	181	242	43	96	196	33	229	37	220	130	60	88	212
13	46	93	44	221	62	87	114	100	75	246	230	222	204	235	19	164
14	128	233	252	117	82	146	138	17	161	191	53	218	166	52	145	23
15	159	108	198	28	92	31	243	207	32	134	244	0	250	152	36	101

Table 2: The Proposed S-box

This step is summarized below. The Chaotic Lorenz system considered in this work can generate three real sequences which we denote as x , y , and z . For the purpose of enhanced randomness, we separate the first 100 values of the real sequences and denote the three real sequences as $\{x_i\}, \{y_i\}, \{z_i\}$, where $i = 1, 2, 3, \dots, m \times n$, where $m \times n$ is the size of plain image. The t^{th} value of the sequences of x , y , and z are defined as x_t, y_t and z_t . We incorporate a disturbing procession in order to evade the appearance of the periodic absolutely. This is done by altering the value of x and y with an interval of 10000:

$$(4.30) \quad \begin{cases} x_t = x_t + 0.1, y_t = y_t - 0.2, & \text{if } z_t \leq 0, t \equiv 1 \pmod{10000}, \\ x_t = x_t + 0.2, y_t = y_t - 0.1, & \text{if } z_t > 0, t \equiv 1 \pmod{10000}. \end{cases}$$

At first, the integral part of the real sequences for all of x , y and z is discarded:

$$(4.31) \quad \begin{cases} x_i = x_i - \text{floor}(x_i), \\ y_i = y_i - \text{floor}(y_i), \\ z_i = z_i - \text{floor}(z_i). \end{cases} \quad i = 1, 2, 3, \dots, m \times n,$$

where $\text{floor}(x)$ means the maximum integer which is smaller than x . Next, a new chaotic sequence is developed as follows:

$$(4.32) \quad k_i = x_i, y_i, z_i, x_{i+1}, y_{i+1}, z_{i+1}, \dots, x_{i+\text{floor}(\frac{m \times n}{3})}, y_{i+\text{floor}(\frac{m \times n}{3})}, z_{i+\text{floor}(\frac{m \times n}{3})}$$

At last, we get the modified chaotic sequence k_i . The beauty of proposed chaotic sequence is that it has the flavor of three x_i, y_i and z_i chaotic sequences of chaotic Lorenz system. During experiment we have changed the length of k_i according to the size of plain image $m \times n$ by discarding some of its values from the end.

In order to get an improved image encryption scheme, we have changed the position of plaintext image pixels by randomness of k_i . The proposed scheme is a two phases scheme.

Pri. poly of $GF(2^8)$	N.L	BIC	BIC of SAC	SAC	LP	DP
$x^8 + x^4 + x^3 + x^2 + 1$	104.75	105.071	0.500	0.493	160/ 0.125	0.125
$x^8 + x^5 + x^3 + x^1 + 1$	105.75	104.929	0.502	0.503	158/ 0.140	0.242
$x^8 + x^5 + x^3 + x^2 + 1$	104.75	101.14	0.502	0.497	168/ 0.156	0.5
$x^8 + x^6 + x^4 + x^3 + x^2 + x^1 + 1$	105.75	105.35	0.502	0.502	160/0.125	0.125
$x^8 + x^7 + x^6 + x^1 + 1$	104.5	104.14	0.498	0.498	164/0.148	0.25
$x^8 + x^6 + x^5 + x^2 + 1$	105.5	105.71	0.502	0.505	160/0.125	0.125
$x^8 + x^7 + x^2 + x^1 + 1$	106.75	104.85	0.503	0.502	160/0.125	0.125
$x^8 + x^7 + x^3 + x^2 + 1$	104.25	104.42	0.501	0.512	162/0.132	0.25
$x^8 + x^7 + x^6 + x^5 + x^4 + x^2 + 1$	106.5	105	0.504	0.496	162/0.132	0.117
$x^8 + x^7 + x^6 + x^5 + x^2 + x^1 + 1$	106.25	103.71	0.500	0.498	162/0.132	0.125
$x^8 + x^6 + x^3 + x^2 + 1$	106	105.71	0.501	0.499	158/ 0.125	0.125
$x^8 + x^7 + x^6 + x^5 + x^2 + x^1 + 1$	106	103.57	0.502	0.497	166/0.156	0.25
$x^8 + x^6 + x^5 + x^1 + 1$	106.5	105.5	0.502	0.510	162/ 0.132	0.125
$x^8 + x^6 + x^5 + x^3 + 1$	106.25	105.37	0.504	0.507	158/0.132	0.125
$x^8 + x^6 + x^5 + x^4 + 1$	107.25	106.07	0.5	0.496	158/0.125	0.117
$x^8 + x^7 + x^5 + x^3 + 1$	106	105.35	0.503	0.516	162/0.132	0.125

Table 3: Analysis of proposed S-boxes with different Primitive polynomial of $GF(2^8)$.

The first phase starts from equation 4.30 and ends at equation 4.34. The basic purpose of first phase is to change the pixel positions of image. The second phase consists of equation 4.35, 4.36 and 4.37 and in this process we are attaining pixel value change based on XOR operation to get a fully encrypted image. Let us assume that the plain image is I with m rows and n columns. For the sake of convinience, we have changed the image I to a one dimensional vector, say $I_1(1 : m \times n)$.

$$(4.33) \quad I_1((p-1)n + q) = I(p, q)$$

where $p = 1, 2, 3, \dots, m$ and $q = 1, 2, 3, \dots, n$. Now, the chaotic sequence k_i , will change the vector I_1 to I_2 with the help of following procedure.

$$(4.34) \quad I_2(i) = I_1(k_i)$$

where $i = 1, 2, 3, \dots, m \times n$. Define a new sequence with elements from $GF(2^8)$ based on k_i as follows.

$$(4.35) \quad l(i) = \text{mod}(\text{round}((k_i \times 10^4)), 256)$$

After getting $l(i)$ sequence of random decimal numbers from $GF(2^8)$, we will XOR $l(i)$ with $I_2(i)$ to get the final vector $I_3(i)$. Reshape $I_3(i)$ in the form of $m \times n$ matrix to get the first level ciphered image as shown in equation 4.37.

$$(4.36) \quad I_3(i) = I_2(i) \oplus l(i)$$

$$(4.37) \quad C.I = \text{reshape}(I_3(i), m, n).$$

As a last step for the proposed algorithm, we have applied the substitution step. We can define the process of substitution in following steps:

1. Consider the pixel of the image in the form of binary byte i.e., 8 binary bits. We divide this set into four LSBs (Least significant bits) and Most significant bits (MSBs).
2. In the next step, the MSBs and LSBs having 4 bits each are converted into decimal values. Conventionally, the pixel value which has to be replaced by S-box value is selected with the help of decimal value of LSBs and MSBs. The S-box column is selected by the decimal value of LSBs whereas the row of S-box is carefully chosen by decimal value of MSBs.
3. One by one all the pixel values are substituted with the values of S-box.
4. In this case, as there are number of S-boxes so each pixel of the image is replaced by single S-box, second pixel value is replaced by another S-box and this procedure will continue till last pixel value.
5. For the selection of S-box out of 256 S-boxes with whom the original value will be replaced is done with the help of x, y, z trajectories of Lorenz map.

5 Simulation results and statistical analysis

For simulation results, we take an image of cameraman having size $256 \times 256 \times 3$. Table 4 represents the initial values of the chaotic maps which are used as secret keys. The plain image and histogram of cameraman are depicted in Fig. 1a and Fig. 1c. Fig. 1a undergoes the process of encryption through our proposed encryption scheme. Fig. 1b gives the encrypted image. The quality of encryption algorithm is exhibited in the strong visual results of encrypted image. Furthermore, the histogram of encrypted image in Fig. 1d also confirms the strength of our scheme. The proposed image encryption scheme is also applied on gray scale image having gray value of 124. The gray scale image is given in Fig. 2a. Fig. 2b represents the encrypted image of the gray scale image. Moreover, Fig. 2c and Fig. 2d depict respectively the histogram images of plaintext image and encrypted image. The encryption results are satisfactory regardless that the plain image is high in autocorrelation. Furthermore, the histogram of the encrypted gray scale image show strength of our proposed technique.

Parameters	a	b	c
	10	28	$\frac{8}{3}$

Table 4: The initial conditions for the chaotic maps utilized as the secret keys in proposed encryption technique.

5.1 Statistical analysis

The purpose of statistical analysis is for assessing the robustness of our designed image encryption technique. We employ distinct statistical analyses to determine the standard of our proposed image encryption technique. In addition to this, the outcomes of our proposed technique are compared with the corresponding results of well-known image encryption methods. The description of these analyses is given in the following subsections.

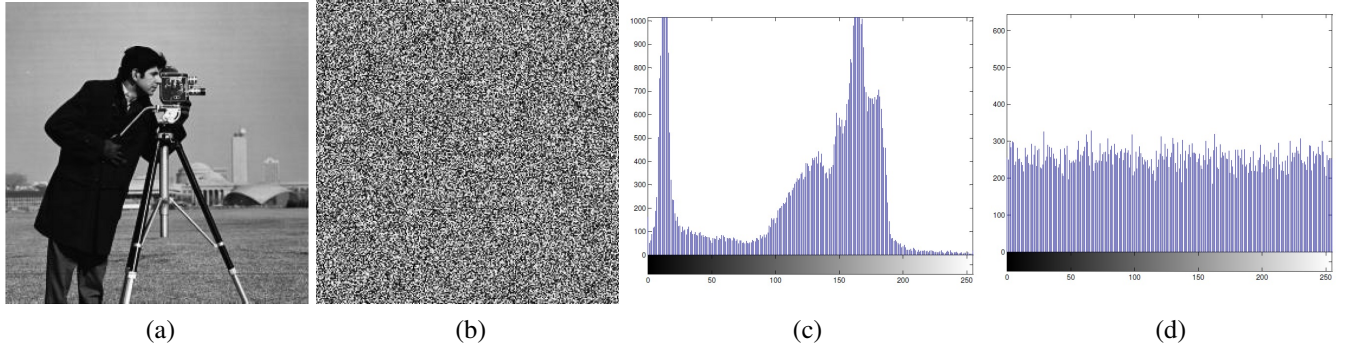


Figure 1: Simulation outcomes of proposed scheme (a) 256×256 size plain image of cameraman (b) cameraman image after encryption with secret keys (c) histogram analysis of cameraman (d) histogram analysis of encrypted cameraman.

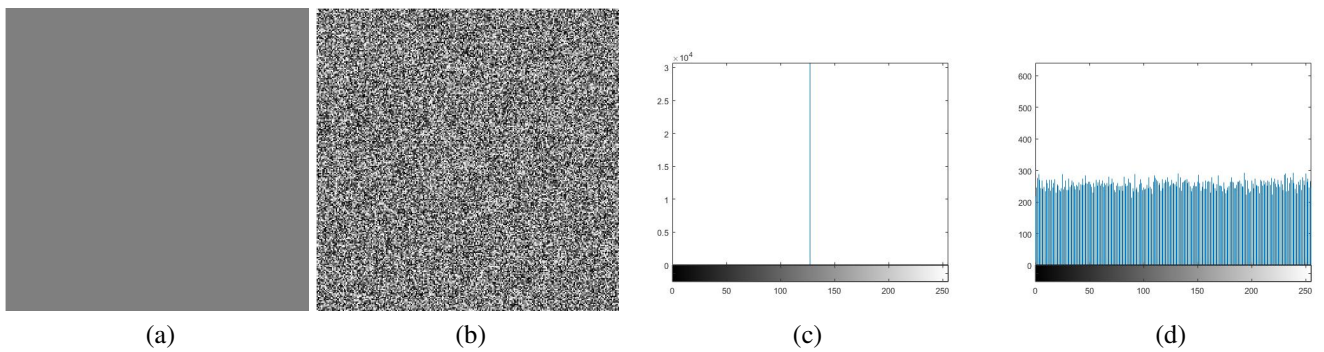


Figure 2: Simulation outcomes of new image encryption technique. (a) gray scale image having 256×256 size, (b) encrypted image (c) histogram results of one gray scale image (d) histogram results of encrypted one gray scale image.

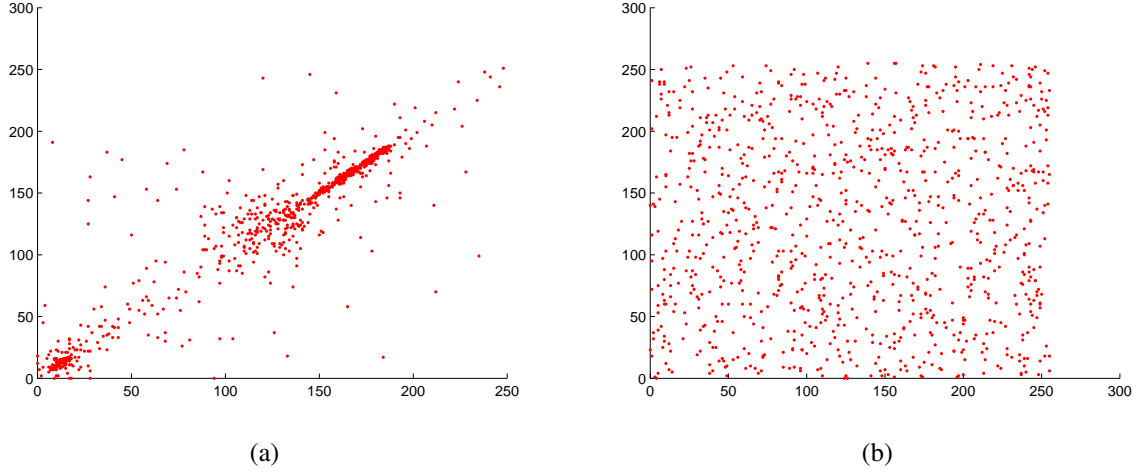


Figure 3: The distribution of horizontally adjacent pixels of (a) cameraman image and (b) encrypted cameraman image. The distribution of vertically adjacent pixels of ciphered cameraman image will have same behavior as pixels that are horizontal adjacent .

5.1.1 Correlation

Given an image with $\rho(i, j)$ representing the pixel value at (i, j) position of the image. The correlation of image is defined by [31] :

$$(5.38) \quad Corr. = \sum_{i,j} \frac{(i - \mu_i)(j - \mu_j)\rho(i, j)}{\phi_i \phi_j}$$

where the standard deviation is denoted by ϕ and μ is the variance. The value of correlation provides a measure of similarity between the two neighboring pixels over the entire image. Its values span is in $[-1, 1]$ where 1 represents perfect correlation.

The distribution of horizontally adjacent pixels of cameraman image is shown in Fig. 3a. Fig. 3b displays the distribution for those pixels of encrypted cameraman image which are horizontally adjacent. The distribution of vertical adjacent pixels in ciphered cameraman image will act similar as they respond in horizontal adjacent pixels.

5.1.2 Entropy

Given an image with $\rho(i, j)$ representing the pixel value at (i, j) position of the image. The entropy of image is defined by [31]:

$$(5.39) \quad Entropy = - \sum_{i,j} pr(\rho(i, j)) \log_2 pr(\rho(i, j)).$$

where $pr(\rho(i, j))$ denotes the probability of image pixel. For an image having 256 gray scales, the entropy values are distributed in $[0, 8]$ and determine the randomness of image. Bigger values of entropy imply bigger measure of randomness.

5.1.3 Contrast

Given an image with $\rho(i, j)$ representing the pixel value at (i, j) position of the image. The contrast of image is defined by [31]:

$$(5.40) \quad Contrast = \sum_{i,j} |i - j|^2 \rho(i, j).$$

The contrast values have the range $[0 (size(Image) - 1)^2]$. In case of a constant image, the contrast value is 0. Bigger values of contrast imply more variation in image pixels. The image contrast analysis makes it possible for the observer to clearly recognize the objects in the image texture.

5.1.4 Homogeneity

In [31], the homogeneity of image is defined by:

$$(5.41) \quad Homo. = \sum_{i,j} \frac{\rho(i, j)}{1 + |i - j|}.$$

where the location of image pixels is given by i, j . In this analysis, the closeness of gray level cooccurrence matrix (GLCM) diagonal and GLCM is calculated. The homogeneity values lie in the interval $[0 1]$.

5.1.5 Energy

The energy of an image can be defined by

$$(5.42) \quad Energy = \sum_{i,j} \rho(i, j)^2.$$

where i, j depicts the position of image pixels. The above equation interprets the energy as the summation of the square of all elements of GLCM. The energy values lies in the interval $[0 1]$ and the constant image has maximum energy value of 1.

Table 5 shows the values of statistical analyses and also the comparison with other existing techniques. This comparison indicates the quality of our proposed scheme.

Analysis	Corr.	Entropy	Homo.	Contrast	Energy
Ref. [32]	-0.0308	7.9311	0.8365	8.0522	0.1984
Ref. [33]	0.0439	2.5643	0.5733	4.9454	0.4263
Ref. [34]	-0.0293	7.9801	0.9102	8.6603	0.0674
Ref. [35]	0.0313	7.9735	0.8251	8.1833	0.2132
Ref. [36]	0.0687	7.1735	0.8121	8.3849	0.1254
Proposed	-3e-4	7.9521	0.9598	8.4587	0.3521

Table 5: Comparison of the statistical analyses of the encrypted images of Lena obtained through application of proposed image encryption algorithm and other relevant techniques.

6 Security analysis

It is mandatory to compute the security analyses to assess the strength of any cryptosystem. Here, we assess the security of our scheme with the help of certain security analyses like key space, key sensitivity, avalanche analysis, noise resistant analysis and cryptanalysis. The comparison of the outcomes of these analyses with the security analyses of other schemes exemplify the strength of our proposed technique. Following sections describe the security analyses in detail.

6.1 Key space and key sensitivity

For any cryptographic system, the total count of secret keys which are utilized to encrypt the data are named as key space and it has its importance as far as security of whole scheme is concerned. In this work, the initial conditions of three different chaotic maps are the secret keys. The secret key has average range of 10^{20} and we have used three different secret keys so the total count of different keys is given as $10^{20 \times 3} = 10^{60}$. A recent personal computer will require over 10^{10} years to go through all possible blends of this huge keyspace.

One of the features of the quality cryptosystem is its sensitivity to a tiny change in secret keys. For instance, the change in secret key during decoding process will give altogether a different decoded image. This mechanism is named as key sensitivity. Our designed encryption technique is sensitive even to a minor variation in the initial conditions. To prove this claim, we will change the secret keys and show the pictorial results. By using secret keys given in Table 4, we have encrypted the cameraman image as given in Fig. 1b. Considering four different cases of changing initial secret keys we have following results.

Case I: If the initial secret key k_1 is slightly changed i.e., $k_1 = a = 10$ to $k'_1 = a = 10.0000000001$ then it is observed that the decryption process does not get the required results. Fig. 4a depicts the decryption of plain-image with key k'_1 . In this process, the remaining two keys were remained the same.

Case II: For the second case, the key k_2 is changed from its original value i.e., $k_2 = b = 28$ to $k'_2 = b = 28.0000000001$ and again with this slight change in one key, the decryption image does not resemble to the original plaintext image and hence prove our claim of key sensitivity. The decryption is given in Fig. 4b.

Case III: The initial secret key k_3 is slightly changed while keeping the remaining keys same. A change of 0.0000000001 in k_3 i.e $k_3 = c = \frac{8}{3}$ to $k'_3 = c = \frac{8}{3} + 0.0000000001$ provides a different original image as given in Fig. 4c.

Case IV: For the last case, the key k_4 is changed like $k_1 = a = 10$ to $k'_1 = a = 9.9999999999$ and the decrypted image is given in Fig. 4d.

For each of the four cases, even a slight variation in the initial secret key could not obtain the original image and hence proving our claim of key sensitivity for proposed algorithm.

6.2 Avalanche analysis

In block ciphers, the effect of avalanche mentions one of the properties of strong cryptographic algorithms. If a single input bit change effect the half number of output bits, then it is an apparent avalanche effect. Researchers prefer unified average change intensity (UACI) and number of pixel change rate (NPCR) to measure the effect of avalanche criteria. The detailed

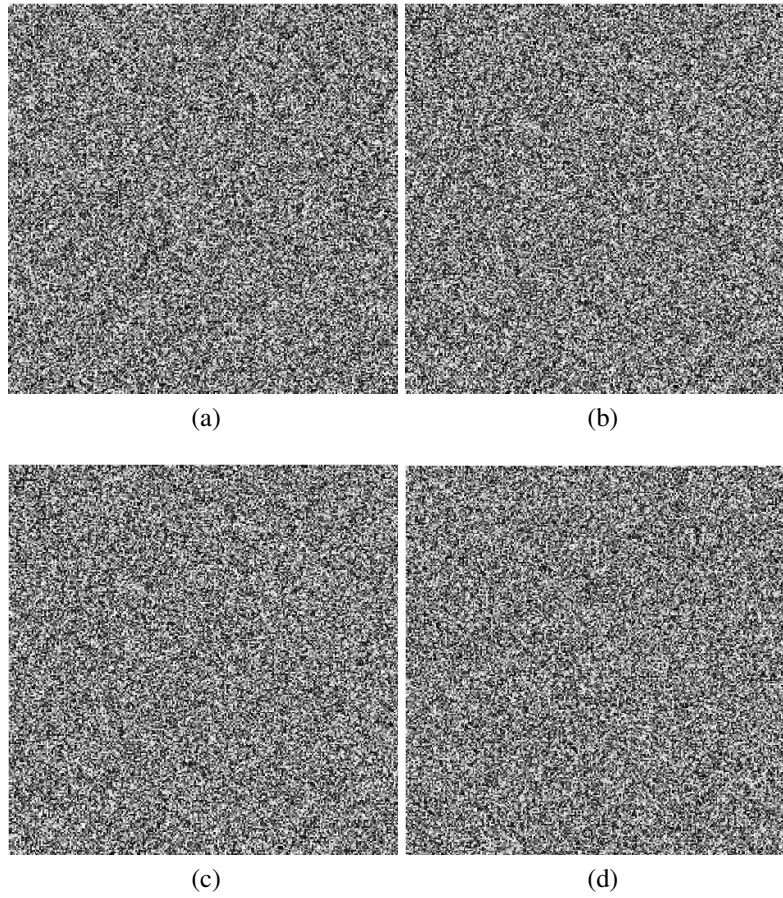


Figure 4: Key sensitivity analysis (a) First secret key is altered from $k_1 = a = 10$ to $k'_1 = a = 10.0000000001$ (b) Second secret key is $k_2 = b = 28$ to $k'_2 = b = 28.0000000001$ (c) Third secret key is altered from $k_3 = c = \frac{8}{3}$ to $k'_3 = c = \frac{8}{3} + 0.0000000001$ (d) Fourth secret key is altered from $k_1 = a = 10$ to $k'_1 = a = 9.9999999999$.

description of this effect is provide in [37] as

$$(6.43) \quad NPCR = \frac{\sum_{i,j} D(i,j)}{N \times M} \times 100\%,$$

$$(6.44) \quad UACI = \frac{1}{N \times M} \left[\sum_{i,j} \frac{|C_1(i,j) - C_2(i,j)|}{255} \right] \times 100\%,$$

where the two ciphered digital images C_1 and C_2 are attained by changing the single bit of plain image. Moreover, the height and width of cipher images are given by N and M respectively. We can define the $D(i, j)$ as

$$D(i, j) = \begin{cases} 0 & \text{if } C_1(i, j) = C_2(i, j), \\ 1 & \text{if } C_1(i, j) \neq C_2(i, j). \end{cases}$$

By adjusting the single pixel of plaintext image, the rate of change of pixel quantity of encrypted image is measured by number of pixel change rate (NPCR) analysis. Moreover, the normal power of contrast between plain and encrypted images is calculated by unified average change intensity analysis (UACI). The calculated minimum value for NPCR must be 50percent. In our work, three different plain images of Lena, baboon and cameraman have been through NPCR and UACI analyses. For each image, the position of bit is firstly changed around first pixel then around middle pixel and finally around the last pixel. Table 6 depicts the outcomes of NPCR and UACI for all cases of three images. In this Table the value of NPCR remains greater than 99 percent and value of UACI is greater than 33 percent. These results indicate the strong avalanche effects. In addition to this, a comparison has been established between avalanche values of proposed scheme and AES

Analysis		UACI(%)		NPCR(%)	
Images & Loc.		Prop.	AES	Prop.	AES
Baboon	first	33.3620	33.4463	99.1252	99.6124
	mid	33.4510	33.4561	99.5271	99.6033
	last	33.6930	33.5252	99.6389	99.6185
Lena	first	33.2010	33.3996	99.2563	99.6094
	mid	33.6320	33.3139	99.5210	99.6506
	last	33.5202	33.5133	99.4198	99.6002
Cman	first	33.5120	33.5360	99.5212	99.6048
	mid	33.3014	33.5212	99.5862	99.6201
	last	33.4120	33.5245	99.5410	99.5819
Key S.	Case I	33.7401	33.5029	99.4802	99.5972
	Case II	33.2015	33.5468	99.0025	99.6460

Table 6: The comparison of UACI and NPCR analysis of our designed technique and AES on images of Lena, Baboon and cameraman. Three cases are proposed for each image which are changing of single bit in the first pixel, the mid pixel and the last pixel. Moreover, the key sensitivity analysis for two cases is given.

By using NPCR and UACI analyses, the key sensitivity of proposed scheme is also evaluated. In first case, two same keys with difference of only 1 bit are used to calculate the difference between two encrypted images. For the second case, the difference of one bit between two keys would remain the same but we calculated the difference between encrypted and decrypted images. Table 6 gives the results of both cases along with comparison with AES. The results of Table show the required avalanche effect.

6.3 Noise resistant analysis

The noise resistant encryption algorithm depicts the strength of any cryptosystem. Any transmitted data may get effected by channel (irrespective of wired or wireless channel) noise or deliberately added noise. It is observed that it is hard to decipher the abandoned cipher image even the portion of the image is affected. Few methods like error detection and correction have been employed to counter these situations but at the cost of computational complexity. For successful transmission and decryption of cipher data, the error detection and correction are required before both the steps. So, ultimately it increases the complexity of the system. In this proposed technique, the addition of noise does not become the hurdle to decipher image correctly with some minor changes. To verify this claim, a series of experiments regarding successful deciphering have been done with noise addition in the cipher images. Fig. 5a and Fig 5b. represent the plain image and encrypted images respectively. This encryption is done with the help of secret keys of Table 4. For noise resistance test, the 10,000 pixels of encrypted image are either cropped or made corrupted with white pixels as illustrated in Fig. 5c. The deciphering of this image is given in Fig. 5d. Clearly, this pictorial representation indicates the successful decryption with minor changes. To prove this claim for other images, the cameraman image is encrypted with the secret keys of Table 4. The plain image with noise and its encryption is given in Fig. 5e and Fig. 5f respectively. Now, again we removed first 10, 000 pixels either with the help of cropping or by corrupting the image. Interestingly, the decryption is successful with minor changes and is shown in Fig. 5h. On the other hand, there is a difference between the deciphering of plain text and digital image. For noisy cipher text, the deciphering of the text gives a whole new text. There are many examples in which the major concern is to recognize the face of the person and object irrespective of quality of decipher images. For this reason, the deciphering of encrypted images having added noise is major breakthrough.

6.4 Cryptanalysis

To assess the strength of proposed scheme against different malicious attacks, following attacks are considered to evaluate the proposed cryptosystem.

6.4.1 Linear cryptanalysis

Linear approximation probability is used to analyze the imbalance of an event. The maximal amount of imbalance of the event can also be obtained with the help of this analysis. In this analysis, two masks Γ_x and Γ_y , respectively are applied to parity of both input and output bits. In [38], it is defined as

$$(6.45) \quad LP = \max_{\Gamma_x \Gamma_y \neq 0} \left| \frac{\{x/X \bullet \Gamma_x = S(x) \bullet \Gamma_y = \Delta y\}}{2^n} - \frac{1}{2} \right|,$$

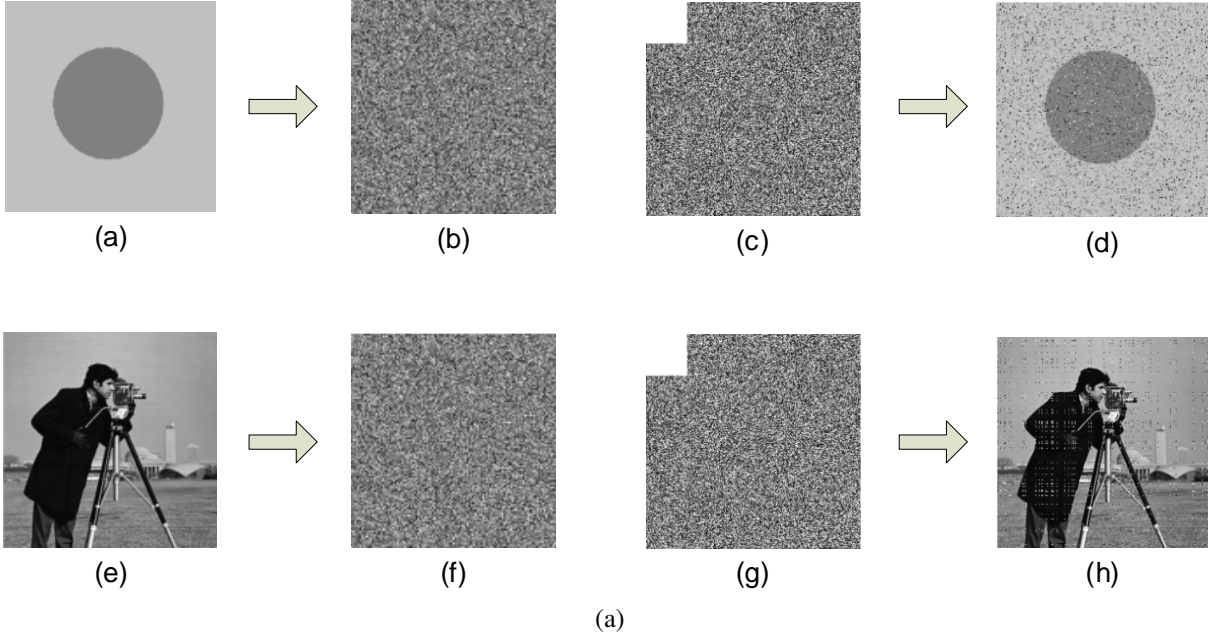


Figure 5: (a) A test image, (b) encryption of test image using secret keys. (c) Adding noise in the cipher image by changing first 10,000 pixels either by cropping or corrupting the file by using the white pixels. (d) Deciphered image. (e) The cameraman noisy image, (f) encryption of cameraman image using secret keys. (g) Adding noise in the cipher image by changing first 10,000 pixels either by cropping or corrupting the file by using the white pixels. After decryption, (h) Deciphered image.

where all the inputs values are contained by set X and total number of this set are 2^n . As we have used 8 different S-boxes and the average maximum value of LP is $LP_{max} = 2^{-4.21}$ and having distinct 256 S-boxes the maximum LP is given as $LP_{max}^{Ar} = 2^{-4.21 \times 256} = 2^{-1077}$. By seeing the outcomes of LP, it is almost impossible for an invader to differentiate our proposed cipher with the help of random permutation and hence, the proposed algorithm will show resistance for countering linear cryptanalysis.

6.4.2 Differential cryptanalysis

One of the precise goals for assurance of uniform mapping, the input differential extraordinarily supervises the differential at output end. These features certify the probability of uniform mapping for every input bit i . The main purpose of approximation probability is to calculate differential uniformity of S-box. In [39] it is given as:

$$(6.46) \quad DP(\Delta x \rightarrow \Delta y) = \left[\frac{\{x \in X/S(x) \oplus S(x \oplus \Delta x) = \Delta y\}}{2^m} \right],$$

where the input and output differentials are given by Δx and Δy respectively. For S-boxes, the maximum average value of DP is $DP_{max} = 2^{-4.05}$. Here, the number of active S-boxes is exactly 256 i.e., $DP_{max}^{Ar} = 2^{-4.05 \times 256} = 2^{-1036}$. By seeing this outcome, it is confirmed that proposed scheme has the ability to resist against malicious differential cryptanalysis.

7 Conclusion

In this paper, a combination of proposed S-boxes and chaotic maps is used for image encryption algorithm. This scheme consists of two phases. In the first phase, substitution is performed via multiple S-boxes instead of a single S-box. The application of several S-boxes not only provides additional security but also utilizes less rounds of encryption. The initial values of Lorenz chaotic map help to operate each round of encryption. In addition to this, permutation is performed in the second phase. The resistance of proposed encryption scheme is depicted through simulation and security analyses results. The outcomes of cryptanalysis also confirm the robustness of our proposed scheme. This work also motivates researchers to add different changes like increasing number of S-boxes and encryption rounds while keeping standard of encryption and computational complexity.

References

- [1] Yang H, Wong K-W, Liao X, Zhang W, Wei P. A fast image encryption and authentication scheme based on chaotic maps. *Commun Nonlinear Sci Numer Simul* 2010;15(11):3507, 17. doi:10.1016/j.cnsns.2010.01.004.
- [2] Yang D, Liao X, Wang Y, Yang H, Wei P. A novel chaotic block cryptosystem based on iterating map with output-feedback. *Chaos Solitons Fractals* 2009;41(1):505, 10. doi:10.1016/j.chaos.2008.02.017.
- [3] Amigo JM, Kocarev L, Szczepanski J. Theory and practice of chaotic cryptography. *Phys Lett Section A* 2007;366(3):211, 16. doi:10.1016/j.physleta.2007.02. 021.
- [4] Jakimoski G, Kocarev L. Chaos and cryptography: block encryption ciphers based on chaotic maps. *IEEE Trans Circuits Syst I* 2001;48(2):163, 9. doi:10. 1109/81.904880.
- [5] Ott E. *Chaos in Dynamical Systems* Second edition 1979.
- [6] Alvarez G, Li S. Some basic cryptographic requirements for chaos-based cryptosystems. *Int J Bifurcation Chaos* 2006;16(08):2129, 51.
- [7] Cicek S, UYAROG LU Y, Pehlivan I. Simulation and circuit implementation of sprott case h chaotic system and its synchronization application for secure communication systems. *J Circuits Syst Comput* 2013;22(04):1350022.
- [8] Pehlivan I, Wei Z. Analysis, nonlinear control, and chaos generator circuit of another strange chaotic system. *Turk J Electr Eng Comput Sci* 2012;20(SUPPL.2):1229, 39. doi:10.3906/elk-1103-14.
- [9] Pareschi F, Setti G, Rovatti R. Implementation and testing of high-Speed CMOS true random number generators based on chaotic systems. *IEEE Trans Circuits Syst I* 2010;57(12):3124, 37. doi:10.1109/TCSI.2010.2052515.
- [10] Ozkaynak F. Cryptographically secure random number generator with chaotic additional input. *Nonlinear Dyn* 2014;78(3):2015, 20. doi:10.1007/ s11071-014-1591-y.

- [11] Wang Y, Wong K-W, Liao X, Chen G. A new chaos-based fast image encryption algorithm. *Appl Soft Comput* 2011;11(1):514, 22. doi:10.1016/j.asoc.2009.12.011.
- [12] Noura H, El Assad S, Vladeanu C. Design of a fast and robust chaos-based crypto-system for image encryption. In: 2010 8th International Conference on Communications, COMM 2010; 2010. p. 423, 6. doi:10.1109/ICCOMM.2010. 5509114.
- [13] Chen G, Mao Y, Chui CK. A symmetric image encryption scheme based on 3D chaotic cat maps. *Chaos Solitons Fractals* 2004;21(3):749, 61. doi:10.1016/j.chaos.2003.12.022.
- [14] Liu H, Kadir A, Niu Y. Chaos-based color image block encryption scheme using S-box. *AEU - Int J Electr Commun* 2014;68(7):676, 86. doi:10.1016/j.aeue.2014. 02.002.
- [15] Dillak RY. Digital color image encryption using RC4 stream cipher and chaotic logistic map. In: Information Technology and Electrical Engineering (ICITEE), 2013 International Conference on; 2013.
- [16] Bakhache B, Ghazal JM, El Assad S. Improvement of the security of zigbee by a new chaotic algorithm. *IEEE Syst J* 2014;8(4):1021, 30. doi:10.1109/JSYST.2013. 2246011.
- [17] Liu Y, Tian S, Hu W, Xing C. Design and statistical analysis of a new chaotic block cipher for wireless sensor networks. *Commun Nonlinear Sci Numer Simul* 2012;17(8):3267, 78. doi:10.1016/j.cnsns.2011.11.040.
- [18] avus oglu U, Akgl A, Kaar S, Pehlivan I, Zengin A. A novel chaos-based encryption algorithm over TCP data packet for secure communication. *Secur Commun Netw* 2016;9(22):5968, 74.
- [19] Jolfaei A, Mirghadri A. Image encryption using chaos and block cipher. *Comput Inf Sci* 2011;4(1):172, 85. www.ccsenet.org/cis.
- [20] Tang G, Liao X, Chen Y. A novel method for designing S-boxes based on chaotic maps. *Chaos Solitons Fractals* 2005;23(2):413, 19. doi:10.1016/j.chaos.2004.04. 023. <http://www.sciencedirect.com/science/article/pii/S0960077904002474>.
- [21] Tang G, Liao X. A method for designing dynamical S-boxes based on discretized chaotic map. *Chaos Solitons Fractals* 2005;23(5):1901, 9. doi:10.1016/j.chaos. 2004.07.033.
- [22] Ozkaynak F, Yavuz S. Designing chaotic S-boxes based on time-delay chaotic system. *Nonlinear Dyn* 2013;74(3):551, 7. doi:10.1007/s11071-013-0987-4.
- [23] Wang Y, Wong KW, Liao X, Xiang T. A block cipher with dynamic S-boxes based on tent map. *Commun Nonlinear Sci Numer Simul* 2009a;14(7):3089-99. doi:10.1016/j.cnsns.2008.12.005.
- [24] Wang Y, Xie Q, Wu Y, Du B. A software for S-box performance analysis and test. In: Proceedings - 2009 International Conference on Electronic Commerce and Business Intelligence, ECBI 2009; 2009b. p. 125, 8. doi:10.1109/ECBI.2009.15.
- [25] Solak E, okal C, Yildiz OT, BIYIKOG LU T. Cryptanalysis of Fridrich chaotic image encryption. *Int J Bifurcation Chaos* 2010;20(05):1405, 13.

- [26] Rhouma R, Solak E, Belghith S. Cryptanalysis of a new substitution-diffusionbased image cipher. *Commun Nonlinear Sci Numer Simul* 2010;15(7):1887, 92. doi:10.1016/j.cnsns.2009.07.007.
- [27] Li S., Mou X and Cai Y. Pseudo-random bit generator based on couple chaotic systems and its applications in stream-cipher cryptography. *Proceedings, Lecture Notes in Computer Science*, 2247, 316-329, 2001.
- [28] Hussain I. A projective general linear group based algorithm for the construction of substitution box for block ciphers. *Neural Computing & Applications*, 22, 1085-1093, 2013.
- [29] Morioka S. An optimized S-box circuit architecture for low power AES design. *Workshop on Cryptographic Hardware and Embedded Systems, CHES.02*, in: LNCS, 2523, 172-186, 2002.
- [30] Hussain I. and Shah T. Literature survey on nonlinear components and chaotic nonlinear components of block ciphers. *Nonlinear Dyn*, 74, 869904 (2013).
- [31] A. Anees, A. M. Siddiqui, J. Ahmed and I. Hussain, "A technique for digital steganography using chaotic maps," *Nonlinear Dynamics*, vol. 75, no. 4, pp. 807-816, Mar. 2014.
- [32] X. Wang, L. Teng and X. Qin, "A novel colour image encryption algorithm based on chaos," *Signal Processing*, vol. 92, no. 4, pp. 1101-1108, Apr. 2012.
- [33] A. Anees, A. M. Siddiqui and F. Ahmed, "Chaotic substitution for highly autocorrelated data in encryption algorithm," *Communications in Nonlinear Science and Numerical Simulation*, vol. 19, no. 9, pp. 3106-3118, Sep. 2014.
- [34] J. Ahmad and S. O. Hwang, "Chaos-based diffusion for highly autocorrelated data in encryption algorithms," *Nonlinear Dynamics*, vol. 82, no. 4, pp. 1839-1850, Dec. 2015.
- [35] X-Y. Wang, L. Yang, R. Liu and A. Kadir, "A chaotic image encryption algorithm based on perceptron model," *Nonlinear Dynamics*, vol. 62, no. 3, pp. 615-621, Nov. 2010.
- [36] A. N. Pisarchika and M. Zaninb, "Image encryption with chaotically coupled chaotic maps," *Physica D: Nonlinear Phenomena*, vol. 237, no. 20, pp. 2638-2648, Oct. 2008.
- [37] Y. Wu, J. P. Noonan and S. Aгаian, "NPCR and UACI randomness tests for image encryption," *Cyber Journals: Multidisciplinary Journals in Science and Technology, Journal of Selected Areas in Telecommunications*, pp. 31-38, 2010.
- [38] M. Matsui, "Linear cryptanalysis of the data encryption standard," *Eurocrypt'93*, LNCS, vol. 765, pp. 386-397, Springer-Verlag, 1994.
- [39] E. Biham and A. Shamir, "Differential Cryptanalysis of the Data Encryption Standard," *Springer-Verlag*, 1993.